

The NN2 Flux Difference Method for Constructing Variable Object Light Curves

Brian J. Barris¹, John L. Tonry¹, Megan C. Novicki¹, and W. Michael Wood-Vasey²

ABSTRACT

We present a new method for optimally extracting point-source time variability information from a series of images. Differential photometry is generally best accomplished by subtracting two images separated in time, since this removes all constant objects in the field. By removing background sources such as the host galaxies of supernovae, such subtractions make possible the measurement of the proper flux of point-source objects superimposed on extended sources. In traditional difference photometry, a single image is designated as the “template” image and subtracted from all other observations. This procedure does not take all the available information into account and for sub-optimal template images may produce poor results. Given N total observations of an object, we show how to obtain an estimate of the vector of fluxes from the individual images using the antisymmetric matrix of flux differences formed from the $N(N - 1)/2$ distinct possible subtractions and provide a prescription for estimating the associated uncertainties. We then demonstrate how this method improves results over the standard procedure of designating one image as a “template” and differencing against only that image.

Subject headings: methods: data analysis — techniques: photometric — supernovae: general

1. Introduction

The astronomical time domain provides unique insight into a range of astrophysical phenomena. Studies of variable stars yield information about stellar structure and evolution

¹Institute for Astronomy, University of Hawaii, 2680 Woodlawn Drive, Honolulu, HI 96822; barris@ifa.hawaii.edu, jt@ifa.hawaii.edu, mnovicki@ifa.hawaii.edu

²Harvard-Smithsonian Center for Astrophysics, 60 Garden Street, Cambridge, MA 02138; wmwood-vasey@cfa.harvard.edu

as well as help to set the extra-galactic distance scale. Active Galactic Nuclei (AGN) reveal the high-energy phenomena associated with the super-massive black holes that reside at the centers of most galaxies. Supernovae (SNe) and Gamma-Ray Bursts (GRBs) provide a glimpse of the fantastic energies released during the violent death throes of several types of stars. Type Ia supernovae (SNe Ia) are of particular interest because their use as “standard candles” has revealed the acceleration of the expansion of the universe from an inferred cosmological constant-like force (Riess et al. 1998; Perlmutter et al. 1999).

Studies of variable sources require specific analysis methods that are not necessary for non-variable sources. Since it is often difficult to detect variation in an object by simply inspecting images, the standard procedure is to subtract images taken at different times to remove objects with constant flux. Photometrically variable objects are then obvious. For the case of SNe, one typically obtains a pair of observations separated in time to allow for SNe not present in the first image to reach observable brightness in the second (see, e.g., Perlmutter et al. 1995 and Schmidt et al. 1998 for a description of the method). After detection, additional observations are made to obtain the complete light curve necessary for cosmological analysis (see Phillips 1993; Riess, Press, & Kirshner 1996). In order to construct the light curve, it is necessary for at least one observation (the “template” image) to contain no SN flux. Often this is the initial image used during discovery of the SN. In many instances, however, the SN is present at a faint level in this image, so an additional observation, taken after the SN has faded from view, is required. The light curve is then calculated by measuring the flux levels in subtractions of each image from the designated template using, for example, the subtraction procedure described by Alard & Lupton (1998). This, the “single-template method,” is the typical means of constructing light curves of SNe and other variable sources.

However, this method has certain drawbacks. The primary flaw is that the quality of any subtraction depends greatly upon the two images involved. If the template is of a poor quality caused, for instance, by poor seeing or a low signal-to-noise ratio (S/N), then *every* subtraction will be degraded, with a corresponding increase in the measured flux uncertainty, even if all other images are of high quality. Any flaw in the template creates a systematic error for the entire light curve that is not detectable from internal consistency checks or through comparison with another SN light curve.

In order to alleviate this problem, we have developed a new method for constructing light curves of photometrically variable objects. Given N observations there are a total of $N(N-1)/2$ pairs of images that can be subtracted together, only $N-1$ of which are performed in the single-template method. A matrix of flux differences can be constructed from these subtractions and used to determine the flux at each individual epoch. This process removes

the dependence on any single observation, because all observations are treated equally as a “template.” We refer to this method as the “ $N(N-1)/2$ ” method (hereafter abbreviated NN2; see Novicki & Tonry 2000 for an initial description).

Section 2 describes the mathematical underpinnings of NN2. In Section 3 we demonstrate the efficacy of the method using simulated SNe inserted into images used during an actual high-redshift SN survey. Section 4 gives our conclusions.

2. Mathematical Basis of the NN2 Method

We assume that we start with N observations of an object, so that one may construct from all pairs of subtractions an $N \times N$ antisymmetric matrix A of flux differences that we wish to analyze as a “vector-term difference.” In other words, we want to find an N -vector V of fluxes such that

$$A_{ij} = V_j - V_i. \quad (1)$$

We also assume that we have a symmetric $N \times N$ error matrix E that expresses our uncertainty in each term of A . As we shall see, this matrix may not be easy to generate, and its interpretation may be somewhat ambiguous. However, one can imagine generating an error matrix by the following procedure.

In each of the difference images, we measure a flux for the object in question. In general this measurement consists of fitting a fixed point-spread function (PSF) profile at the location of the object by adjusting the amplitude of the PSF (both positive or negative) and the local background level. The PSF profile may be obtained from a suitable star in the original image while the location of the variable source may be determined by summing all the difference images (adjusted to keep the sign of the object positive) and fitting the location in this sum. Once we have a flux measurement, we can insert copies of the object at nearby empty regions of the difference image and repeat the procedure. The mean of the recovered fluxes indicates whether there is a bias in the measurement, and the scatter may be used as a term E_{ij} in the error matrix.

The crux of the NN2 method is the distillation of the photometric measurements from the full set of $N(N-1)/2$ subtractions to a lightcurve, V , that represents our best understanding of the behavior of the object under consideration. As long as it is consistent, the exact procedure for measuring the flux on the difference images is not central to the NN2 method we present here.

In order to find an optimal V , we wish to minimize the quantity

$$\chi^2 = \sum_{i,j;i < j} \frac{(-A_{ij} + V_j - V_i)^2}{E_{ij}^2} \quad (2)$$

This construction may not be entirely appropriate depending on the errors in the flux differences A_{ij} . Ideally, if we possessed an extremely high-quality template with no SN flux present and applied an optimal subtraction procedure, the errors would be primarily due to photon counting statistics (see Alard & Lupton 1998 for a discussion). We would expect these errors to be uncorrelated and would simply wish to employ the single-template method to construct the SN light curve. As mentioned in the introduction, in practice there are nearly always imperfections associated with the template image that remove us from this idealized regime. These template errors introduce correlations in the individual flux measurement errors that are difficult to quantify and are typically assumed to be negligible in SN light-curve analysis. The use of the NN2 method, however, will introduce further correlations as a result of the common images in the various subtractions (for instance, the error in $V_1 - V_2$ will be anti-correlated with the error in $V_2 - V_3$ due to the common error in V_2). Although we believe that the use of the NN2 method will improve the ability to accurately recover variable object light curves, one should recognize that the NN2 method is expected to introduce these additional correlations to the fluxes measured from the various subtraction images, and so the χ^2 given above is not technically appropriate. Errors due to systematics in the subtraction procedure, such as those associated with template or software imperfections, would be expected to be effectively uncorrelated, and if they were dominant then Eq. 2 would indeed represent the proper χ^2 . With these caveats in mind, we will proceed to use the definition of χ^2 as given in Eq. 2 as the basis of the NN2 method. Tests of its ability to recover accurate light-curve information in the following section demonstrate its effectiveness in practice.

However, we need to make one minor modification to our χ^2 because the χ^2 defined in Eq. 2 is degenerate to the addition of a constant to the V vector—geometrically, χ^2 is constant along the line $\sum \hat{i}$. In order to lift this degeneracy and permit us to solve for V , we add a term to χ^2 that is quadratic in the degenerate direction, so that

$$\chi^2 = \sum_{i,j;i < j} \frac{(-A_{ij} + V_j - V_i)^2}{E_{ij}^2} + \frac{(\sum_i V_i)^2}{\langle E \rangle^2}, \quad (3)$$

where $\langle E \rangle$ is a suitable typical uncertainty; for example,

$$\frac{1}{\langle E \rangle^2} = \frac{2}{N(N-1)} \sum_{i,j;i < j} \frac{1}{E_{ij}^2}. \quad (4)$$

Our solution will therefore have $\sum_i V_i = 0$. This construction explicitly forces one to determine an accurate zero flux level at a later stage. In the single-template method this zero flux level is generally implicitly determined by assuming that the object of interest has zero flux in the template image. This same assumption can similarly be used in the NN2 method, but more sophisticated methods involving comparisons of many different images can also be invoked. If the absolute brightness of the variation being studied is important, the NN2 method clearly cannot free one from the requirement of having a fiducial image to measure the zero flux level. This is a fundamental limitation of any differential photometry method as the information is simply not available without such a fiducial image. However, even in the absence of a fiducial image, the NN2 method will produce a sensible and accurate relative lightcurve.

We now seek to solve for our lightcurve vector V by minimizing χ^2 with respect to V :

$$0 = \frac{\partial \chi^2}{\partial V_k} \quad (5)$$

$$= 2 \sum_{i,j;i < j} \frac{(-A_{ij} + V_j - V_i)}{E_{ij}^2} (\delta_{jk} - \delta_{ik}) + 2 \sum_i \frac{V_i}{\langle E \rangle^2}. \quad (6)$$

Exploiting the antisymmetry of A and the symmetry of E we can rewrite Eq. 6 as

$$0 = 2 \sum_{i;i \neq k} \frac{(-A_{ik} + V_k - V_i)}{E_{ik}^2} + 2 \sum_i \frac{V_i}{\langle E \rangle^2}. \quad (7)$$

These N equations can be solved for V by inverting a matrix C :

$$\sum_{i;i \neq k} \frac{A_{ik}}{E_{ik}^2} = \sum_i C_{ik} V_i \quad (8)$$

where

$$C_{ik} = \frac{-1}{E_{ik}^2} + \sum_j \frac{1}{E_{kj}^2} \delta_{ik} + \frac{1}{\langle E \rangle^2}. \quad (9)$$

The inverse of this curvature (Hessian) matrix C yields uncertainties for V from the square root of the diagonal elements as well as covariances from normalizing the off-diagonal elements by the two diagonal terms (under the assumption that the error matrix truly does represent Gaussian, independent uncertainties for each of the terms of the antisymmetric difference matrix).

An alternative approach to calculating uncertainties in V stems from assuming that there is a vector σ such that

$$E_{ij}^2 = \sigma_i^2 + \sigma_j^2. \quad (10)$$

Under this assumption, we seek to minimize

$$\chi_e^2 = \sum_{i,j;i < j} (-E_{ij}^2 + \sigma_i^2 + \sigma_j^2)^2. \quad (11)$$

The minimization condition is

$$0 = \frac{\partial \chi_e^2}{\partial \sigma_k^2} \quad (12)$$

$$= 2 \sum_{i,j;i < j} (-E_{ij}^2 + \sigma_i^2 + \sigma_j^2) (\delta_{ik} + \delta_{jk}) \quad (13)$$

$$= 2 \sum_{i;i \neq k} (-E_{ik}^2 + \sigma_i^2 + \sigma_k^2). \quad (14)$$

These N equations are solved by inverting a matrix D

$$\sum_{i;i \neq k} E_{ik}^2 = \sum_i D_{ik} \sigma_i^2 \quad (15)$$

where

$$D_{ik} = 1 + (N - 2)\delta_{ik}. \quad (16)$$

After solving for V and σ , we can evaluate the quality of the fit by comparing χ^2 to the number of degrees of freedom,

$$N_{\text{dof}} = \frac{N(N - 1)}{2} - (N - 1). \quad (17)$$

This N_{dof} comes from the number of data points, $N(N - 1)/2$, minus the number of model parameters, $N - 1$. Recall that we’ve explicitly required $\sum_i V_i = 0$, so that the number of model parameters is $N - 1$ rather than N .

Having outlined the basic method, we now discuss a fundamental uncertainty in the NN2 process. We can imagine two types of error that will cause V to differ from the true flux values. The first, which we term “external error,” is intrinsic to the images themselves. For example, if the object has a positive statistical fluctuation in flux in one image or is corrupted by a cosmic ray that happens to coincide with the position of the object on the detector, this error will propagate through the entire differencing and analysis procedure. It is possible to obtain an antisymmetric difference matrix that is an exact vector-term difference ($\chi^2 = 0$), but the solution vector will still contain errors. The second type of error, which we call “internal error,” is caused by the procedure of generating the antisymmetric matrix. One might imagine a set of images that have no flux error whatsoever, but through errors in

convolving, differencing, or flux fitting, an antisymmetric matrix may be created that is not a perfect vector-term difference and for which $\chi^2 > 0$.

Roughly speaking, one might expect that if the error matrix E consists entirely of external errors the resulting σ terms will all be approximately $E/\sqrt{2}$, since E is the quadrature sum of two σ terms. Alternatively, if the error matrix is purely internal error the σ terms might be expected to be approximately E/\sqrt{N} , since each term in V comes from comparison with $N - 1$ other images. In the case of external errors, the uncertainties derived from the χ_e^2 analysis are correct. In the internal error case the uncertainties obtained from the covariance matrix derived from the χ^2 analysis are likewise appropriate.

It is not clear how to disentangle these different sorts of errors. The procedure suggested above of dropping copies of the object into each difference image and evaluating the scatter of the result will be sensitive to each sort of error, but it is possible to imagine cases where this procedure is unsatisfactory. We suggest that the errors provided in the E matrix be interpreted as external errors and taken seriously as such. Thus, the vector V is assigned an external uncertainty equal to the σ vector. However, in order to handle a situation where χ^2/N_{dof} is much greater than 1 (i.e., where the antisymmetric matrix is simply *not* well represented as a vector-term difference), we suggest also creating an internal uncertainty vector τ that is obtained from the diagonal terms of the covariance matrix, scaled by χ^2/N_{dof} :

$$\tau_k = \left(C_{kk}^{-1} \frac{\chi^2}{N_{\text{dof}}} \right)^{1/2} \quad (18)$$

The total uncertainty is then the quadrature sum of σ and τ . Note that this approach implicitly assumes that the internal and external errors are uncorrelated and are proportional to one another as well as the provided E matrix.

For problems where χ^2/N_{dof} is near unity without adjustment, the τ vector will be smaller than the σ vector by approximately $\sqrt{2/N}$ and will make a fairly small contribution to the total uncertainty. When $\chi^2/N_{\text{dof}} \ll 1$ (i.e., the antisymmetric matrix is very closely represented by the vector-term difference), the τ vector will be negligible. However, when $\chi^2/N_{\text{dof}} \gg 1$, the τ vector will act to correct χ^2/N_{dof} to approximately unity, and this procedure will provide reasonable uncertainties, even though E may be much too small.

3. Demonstration of Improved Accuracy in Recovering Variable Object Light Curves

The first extensive use of the NN2 method we have developed here occurred during the SN-search component of the IfA Deep Survey (Barris et al. 2004), although we also employed it to a limited extent in a previous SN survey by Tonry et al. (2003). The IfA Deep Survey was undertaken primarily with Suprime-Cam (Miyazaki et al. 1998) on the Subaru 8.2-m telescope and was supplemented with the 12K camera (Cuillandre et al. 1999) on the Canada-France-Hawaii 3.6-m telescope. Scores of high-redshift SN candidates were discovered (Barris et al. 2001, 2002) with 23 confirmed as SNe Ia. We here present several tests we performed to demonstrate the improved performance of NN2 relative to the single-template method.

In order to make a controlled test of the effectiveness of NN2 vs. the single-template method, we inserted artificial SNe into the survey images. The light curves of these objects consisted of a linear ramp-up and ramp-down in brightness over the time period covered by the survey observations. The timing of the light-curve maxima were selected at random and could lie within or outside of the survey period. The simulated SNe were laid down in a regular grid across the survey area, and all pairs of images were subtracted. Object-detection software was then run on all subtraction images to detect photometrically variable objects (both real objects and the artificial SNe) and to construct the NN2 flux difference matrix. The positions of both real and artificial SNe were fit by the object-detection software as described in Section 2. Since we knew the true light-curve properties used to create the synthetic SNe, we could calculate the root-mean-square scatter (RMS) around this artificial light curve using both the NN2 flux calculation and the single-template method with every individual observation as the template (this latter is equivalent to taking the flux values from a single column of the NN2 flux difference matrix).

We inserted approximately 2000 simulated SNe into the *I*-band observations of each of four ~ 0.5 square-degree fields from the IfA Deep Survey, spanning a peak magnitude range of approximately $m_I = 21$ – 25 . We used a predefined grid of positions to insert the simulated SNe, without taking into consideration the presence of actual objects nearby that would cause problems for detection and accurate photometric measurements. The small fraction that were so affected were accordingly not used in the final analysis.

Figure 1 shows the percentage improvement in the cumulative distributions of the RMS (in flux units) from the NN2 method over the set of all RMS values from the single-template method from the four survey fields (RMS values are calculated from flux measurements scaled so that a value of flux = 1 corresponds to a magnitude of 25). The cumulative fraction for the NN2 method is larger than that for the single-template method distribution at all values

of RMS, indicating that the NN2 method does indeed tend to yield *smaller* RMS values. The NN2 method more accurately recovers the actual light curve of these variable objects.

Since one could imagine that certain templates of very high quality could outperform the NN2 method while the collection of all single-template measurements, as shown in Fig. 1, does not, we next examine the relationship between the NN2 RMS and the single-template RMS for individual observations. To illustrate this comparison, we will concentrate on only one of the survey fields, although details of our investigation of the entire survey area can be found in Barris (2004). Table 1 contains relevant information for the 16 observations of the selected field, f0438. This field is representative of the entire survey area, though it is notable that it contains an observation that was quite strongly affected by clouds (Observation 4), as seen by its unusually bright zero-point magnitude. Also noteworthy is Observation 11, taken in poor seeing conditions. We would expect the performance of the single-template method using these observations to be poor in comparison to the NN2 procedure.

In Table 1 we demonstrate that the typical RMS obtained with the NN2 method for the set of 1775 simulated SNe is smaller than the single-template method RMS using *every* observation of the selected field. The improvement is generally fairly small, ranging from $\sim 5 - 10\%$. We demonstrate below that these differences are statistically significant. The use of either Observations 4 and 11 as single templates, as expected, produces substantially worse results relative to the NN2 method than the other observations. For these observations the improvement due to the NN2 method is substantially larger than 10%. Figure 2 shows graphically the percentage difference in the cumulative RMS distributions, similar to Figure 1, for each individual observation of f0438.

Having demonstrated the improved performance of the NN2 method, we can test the statistical significance of the differences between the NN2 RMS values and those calculated via the single-template method and examine whether these differences indicate an actual difference in the distributions of the results from the two methods. To do so we use the non-parametric Kolmogorov-Smirnov (K-S) test, with results given in Table 2. For the sample of all single-template RMS values compared to NN2, the K-S probability value is $\lesssim 5 \times 10^{-9}$, indicating with strong confidence that the distributions are different. We also divide the sample into magnitude bins, since the relative behavior of NN2 RMS to single-template RMS is expected to be sensitive to the object’s S/N and hence to the magnitude for a given sensitivity.

The K-S probability values for three approximately equal magnitude bins show that for each of the subsamples the difference between NN2 and the single-template method is statistically significant, increasingly so at fainter magnitudes. Finally, we compare each observation individually with the NN2 method and see again that the observed improvement

in RMS with NN2 is highly significant for nearly all observations (the only obvious potential exception is observation 8). These K-S probability values demonstrate that the NN2 method is not distributed identically to the single-template method, and the differences in median values given in Table 1 are indeed indicative of statistically significant differences in the distributions. This test confirms that the NN2 method truly does produce improved results in generating differential light curves.

4. Conclusions

We have described the mathematical foundation of a new method for constructing the light curves of photometrically variable objects. This method uses all $N(N - 1)/2$ possible subtractions involving N images in order to calculate a vector of fluxes of the variable object and offers a powerful alternative to the single-template method that is in standard use for studying variable sources.

If one has a data set with a limited number of good fiducial observations, the NN2 method will outperform any single-template subtraction approach. For cases where a large number of fiducial observations are available to construct a deep template image, the NN2 method and the single-template approach using this deep template should yield comparable results. In this situation we would encourage the use of both methods to provide additional checks and constraints on the differential light curve.

We have tested the performance of the NN2 method by inserting artificial SNe into images from the IfA Deep Survey and comparing the RMS scatter from flux measurements using the two different methods. We find that the RMS from the NN2 method is better than the single-template RMS for the large majority (typically 65%–72%) of the SNe for every possible template. The median values for the ratio of NN2 RMS (in flux units) to single-template RMS measurements are typically 0.93–0.96, demonstrating that the NN2 method results in a $\sim 5\%$ improvement in the accuracy of the recovered light curve for these observations.

Using Kolmogorov-Smirnov statistics, we have demonstrated that these differences are significant, reflecting an actual difference between the performance of the two methods. We find extremely high probabilities that the NN2 RMS is distributed significantly differently from the single-template RMS values. This difference and improvement in RMS holds even for the very high quality templates that would be considered ideal for the single-template method.

We therefore make the following conclusions:

1. For the IfA Deep Survey observations, use of the NN2 method typically results in a 5-10% improvement in the RMS of the recovered light curve in comparison to the single-template method.

2. For observations that have a large external error, such as those taken under poor conditions, the NN2 method results in a substantial improvement ($\gg 10\%$) over the single-template method.

3. When working with high-quality observations, with small external error, the internal errors (such as those due to implementation of the subtraction process) dominate. If these errors are large, the NN2 method should outperform the single-template method to a large degree. If these errors are kept small, as we believe is possible based on our extensive experience with SN surveys, then the NN2 method will result in a modest but significant improvement in accuracy of light-curve recovery.

In summary, the NN2 method we present here maximizes the time variability information contained in a series of observations by using the relative differences between all pairs of images to construct the optimal differential light curve. references

The source code for our implementation of the NN2 method presented here is available at <http://www.ctio.noao.edu/essence/nn2/>.

This work was supported in part by grant AST-0443378 from the United States National Science Foundation.

REFERENCES

- Alard, C., & Lupton, R. H. 1998, *ApJ*, 503, 325
- Barris, B., et al. 2001, *IAU Circ.* 7745, 7755, 7767, 7768
- Barris, B., et al. 2002, *IAU Circ.* 7801, 7802, 7805, 7806, 7849
- Barris, B.J., et al. 2004, *ApJ*, 602, 571
- Barris, B.J. 2004, Ph.D. thesis, University of Hawaii
- Cuillandre, J-C., et al. 1999, *CFH Bull.* 40
- Miyazaki, S., et al. 1998, in *Proc. SPIE*, 3355, 363
- Novicki, M. C., & Tonry, J. 2000, *BAAS*, 32, 1576
- Perlmutter, S., et al. 1995, in *Thermonuclear Supernovae*, ed. P. Ruiz-Lapuente, R. Canal, & J. Isern (NATO ASI Ser. C, 486) (Dordrecht: Kluwer), 74
- Perlmutter, S., et al. 1999, *ApJ*, 517, 565
- Phillips, M.M. 1993, *ApJ*, 413, L105
- Riess, A.G., Press, W.H., & Kirshner, R.P. 1996, *ApJ*, 473, 88
- Riess, A.G., et al. 1998, *AJ*, 116, 1009
- Schmidt, B.P., et al. 1998, *ApJ*, 507, 46
- Tonry, J.L., et al. 2003, *ApJ*, 594, 1

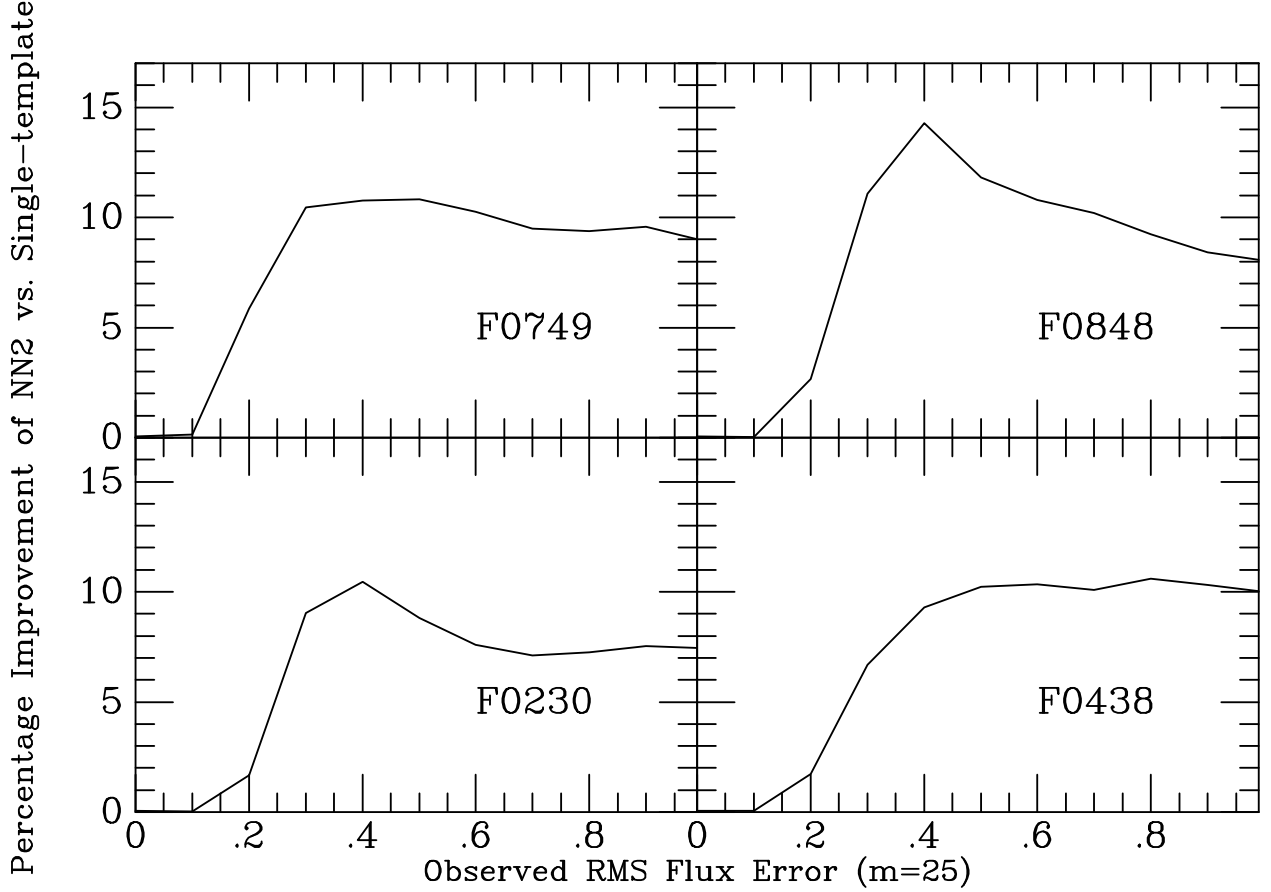


Fig. 1.— The improvement in the cumulative RMS distribution for the NN2 technique compared with that of the single-template method for each of four survey fields is shown here as the extra fraction of NN2-derived light curves, compared to the conventional light curves, that have an observed RMS flux error less than the abscissa value. For each field the NN2 cumulative fraction is larger at all RMS values, demonstrating its improved performance in accurate light-curve recovery compared to the single-template method.

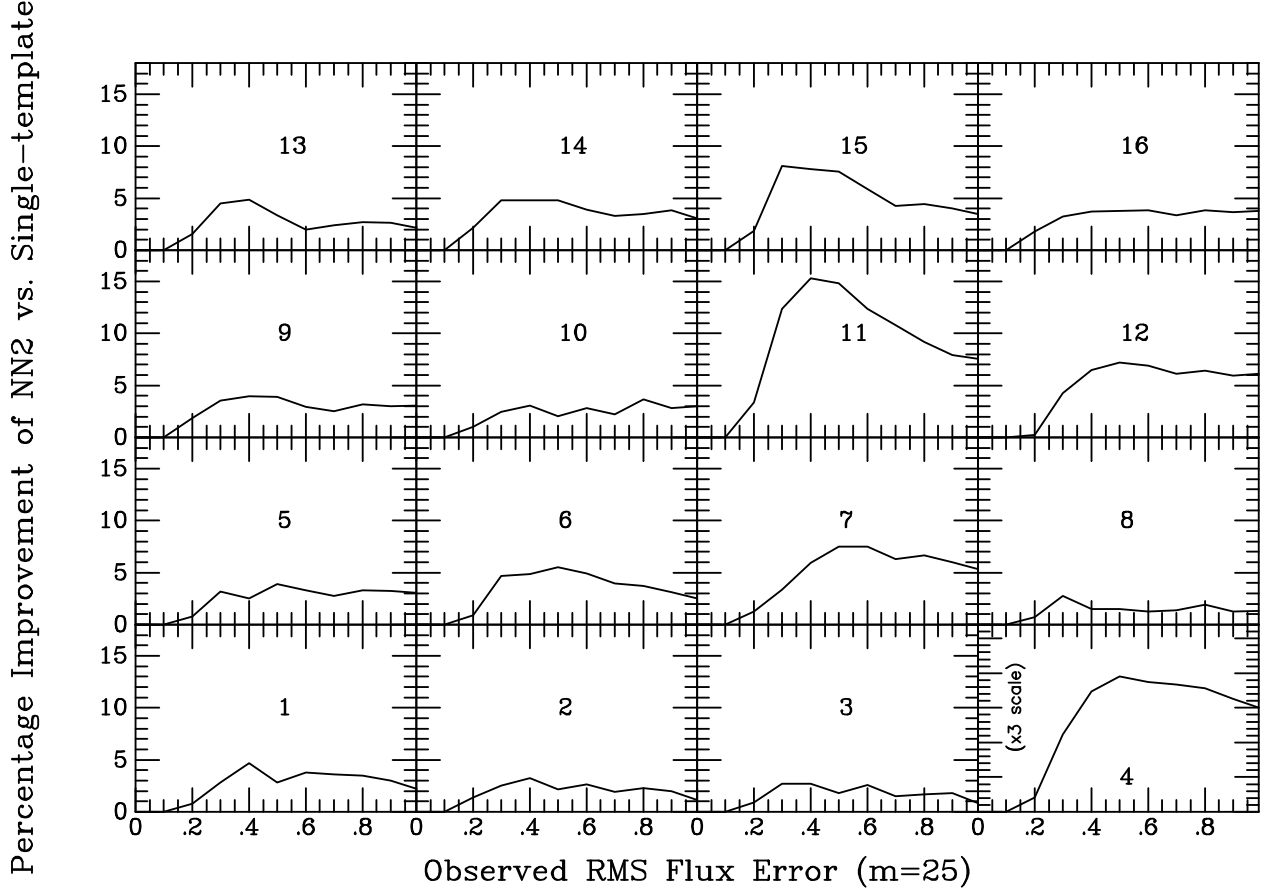


Fig. 2.— The percentage improvement in the cumulative RMS distribution for the NN2 technique compared with that of the single-template method for each of the 16 observations of a representative field, f0438, is shown here as in Fig. 1. Particularly noteworthy are the poor results of using as the single template either observations 4 or 11, which suffered from heavy cloud cover and poor seeing, respectively. The vertical scale of the sub-plot for Observation 4 has been accordingly scaled up by a factor of 3. For templates of higher quality, the difference in relative performance is less significant. Nonetheless, NN2 outperforms the single-template method for any choice of the single template image.

Table 1. F0438 Observational Information and Light-Curve Recovery Comparison

Obs. no.	MJD	seeing ¹	ZP ²	Median RMS ³	Median(RMS _{NN2} /RMS _{temp.}) ⁴
1	52164.57	0.75	30.48	0.441	0.951
2	52176.49	0.72	30.05	0.432	0.963
3	52191.50	0.71	30.12	0.427	0.970
4	52198.56	0.59	27.63	0.810	0.625
5	52204.59	0.63	30.46	0.424	0.973
6	52225.39	0.62	30.17	0.445	0.960
7	52231.38	0.51	30.46	0.455	0.944
8	52232.35	0.68	30.21	0.419	0.970
9	52236.34	0.94	30.36	0.440	0.938
10	52252.35	0.83	30.59	0.429	0.957
11	52263.38	1.14	30.33	0.515	0.839
12	52283.39	0.68	30.51	0.460	0.946
13	52288.23	0.84	30.65	0.438	0.941
14	52289.39	0.93	30.27	0.448	0.936
15	52323.35	0.97	30.23	0.468	0.908
16	52369.25	0.58	29.58	0.432	0.943

¹Arcseconds

²Magnitude zero-point of the processed images from each observation

³RMS calculated for flux units, with flux=1 corresponding to $m = 25$. Median RMS value for the NN2 method is 0.422.

⁴Median value of the ratio of the RMS as calculated with the single-template method to the RMS as calculated with the NN2 method. A total of 1775 simulated SNe were inserted in the survey images for this field.

Table 2. Field 0438 Kolmogorov-Smirnov Statistics

N1	N2	cut criterion	K-S statistic	K-S probability ¹
1775	28400	all	0.0769	4.7430e-09
482	7712	$m < 23.0$	0.0809	4.9083e-03
617	9872	$23.0 \leq m \leq 24.5$	0.0897	1.5707e-04
676	10816	$24.5 < m$	0.1330	2.5150e-10
1775	1775	observation 1	0.0524	1.4698e-02
1775	1775	observation 2	0.0462	4.3869e-02
1775	1775	observation 3	0.0411	9.6888e-02
1775	1775	observation 4	0.3977	<1.0e-30
1775	1775	observation 5	0.0445	5.7717e-02
1775	1775	observation 6	0.0608	2.6510e-03
1775	1775	observation 7	0.0845	5.6244e-06
1775	1775	observation 8	0.0332	2.7611e-01
1775	1775	observation 9	0.0518	1.6326e-02
1775	1775	observation 10	0.0417	8.9127e-02
1775	1775	observation 11	0.1639	2.5672e-21
1775	1775	observation 12	0.0794	2.4901e-05
1775	1775	observation 13	0.0575	5.4234e-03
1775	1775	observation 14	0.0710	2.4226e-04
1775	1775	observation 15	0.0885	1.6592e-06
1775	1775	observation 16	0.0541	1.0650e-02

¹The probability that identically distributed distributions will exhibit a value for the K-S statistic larger than that observed.